Title

Internalization and TLR-dependent type I interferon production by monocytes in response to Toxoplasma gondii

Journal

Immunology and Cell Biology, 92(10)

ISSN

0818-9641

Authors

Han, Seong-Ji
Melichar, Heather J
Coombes, Janine L
et al.

Publication Date

2014-11-01

DOI

10.1038/icb.2014.70

Peer reviewed

Immunol Cell Biol. Author manuscript; available in PMC 2015 May 01.

Published in final edited form as:
Immunol Cell Biol. 2014 November ; 92(10): 872–881. doi:10.1038/icb.2014.70.

Internalization and TLR-dependent type I interferon production by Inflammatory monocytes to *Toxoplasma gondii*

Seong-Ji Han[a,*], **Heather J. Melichar**[a], **Janine L. Coombes**[a,**], **Shiao Wei Chan**[a], **Anita A. Koshy**[b,***], **John C. Boothroyd**[c], **Gregory M. Barton**[a], and **Ellen A. Robey**[a,#]

[a]Division of Immunology and Pathogenesis, Department of Molecular and Cell Biology, University of California, Berkeley, CA, USA.

[b]Department of Medicine (Infectious Disease) and Department of Neurology, Stanford University School of Medicine, Stanford, California, USA.

[c]Department of Microbiology and Immunology, Stanford University School of Medicine, Stanford, California, USA.

Abstract

The classic anti-viral cytokine interferon-β (IFN-β) can be induced during parasitic infection, but relatively little is know about the cell types and signaling pathways involved. Here we show that inflammatory monocytes (IMs), but not neutrophils, produce IFN-β in response to *T. gondii* infection. This difference correlated with the mode of parasite entry into host cells, with phagocytic uptake predominating in IMs and active invasion predominating in neutrophils. We also show that expression of IFN-β requires phagocytic uptake of the parasite by IMs, and signaling through Toll-like receptors (TLRs) and MyD88. Finally, we show that IMs are major producers of IFN-β in mesenteric lymph nodes following *in vivo* oral infection of mice, and mice lacking the receptor for type I interferon (IFN-1) show higher parasite loads and reduced survival. Our data reveal a TLR and internalization-dependent pathway in IMs for IFN-β induction to a non-viral pathogen.

Keywords

parasite; interferon-β; Toll-like receptor; phagocytosis; monocyte

[#]to whom correspondence should be addressed: Ellen Robey University of California, Berkeley Department of Molecular & Cell Biology 142 Life Sciences Addition, #3200 Berkeley, CA 94720-3200 Phone: (510) 642-8669 Fax: (510) 643-9500 erobey@berkeley.edu.

[*]Current address: Program in Barrier Immunity and Repair, Mucosal Immunology Section, Laboratory of Parasitic Diseases, National Institute of Allergy and Infectious Diseases (NIAID), National Institutes of Health (NIH), Bethesda, Maryland, USA.

[**]Current address: Institute of Infection & Global Health, Liverpool Science Park IC2, University of Liverpool, Liverpool, Merseyside L3 5RF, United Kingdom.

[***]Current address: Department of Neurology, Department of Immunobiology, and BIO5 Institute, University of Arizona College of Medicine, Tucson, Arizona, USA.

The authors have no conflict of interest to disclose.

Europe PMC Funders Author Manuscripts

INTRODUCTION

Infection with a wide variety of pathogens can trigger type I interferon (IFN-1) induction in mammalian hosts. Most of our information about the IFN-1 response, however, comes from viral infection models, and the mechanism of induction to non-viral infection remains relatively unexplored. The intracellular protozoan parasite, *Toxoplasma gondii*, provides an ideal pathogen to address this question, as it is an important opportunistic pathogen of humans with relevance to related protozoan parasites including *Plasmodium* and *Cryptosporidium*, and provides a tractable experimental pathogen that allows for physiological oral infection studies in one of its natural hosts, the mouse.

The induction of IFN-1, as well as pro-inflammatory cytokines such as TNF-α and IL-12, is initiated when pathogen associated molecular patterns (PAMPs) are detected by innate immune sensors, including the Toll-like receptor family (TLRs). Multiple TLRs contribute to the host defense during *T. gondii* infection [1-3]. Moreover, different TLRs acting in different host cell types can evoke distinct immune responses to *T. gondii*. For example, TLR11 and TLR12 play a key role in IL-12 production by conventional dendritic cells (cDCs) and macrophages [3-5], TLR2 and TLR4 are required for TNF-α production by macrophages [6, 7], and plasmacytoid DCs (pDCs) produce IFN-β through the activation of TLR12 [3]. Production of IFN-1 can require distinct intracellular signaling pathways, as exemplified by the requirement for endosomal trafficking for type I interferon production but, but not TNF-α, production, following TLR4 triggering 1 [8-11]. The cell types, innate immune pattern recognition receptors, and intracellular trafficking requirements for IFN-1 production during *T. gondii* infection require further study.

PAMPs can be detected at the cell surface, in vacuolar compartments, and in the cytosol of host cells, and the subcellular location can have a profound impact on the nature of the host response [11]. As *T. gondii* invades a cell, it directly injects proteins into the host cell, and invasion culminates in the formation of a specialized parasitophorous vacuole within which the parasite replicates and from which it also releases proteins into the host cell. In addition, during *in vivo* infection, material from parasites could also be released into the extracellular space or taken up by phagocytes. Thus, parasite PAMPs could potentially engage pattern recognition receptors at multiple cellular locations. In addition to providing a potential source of PAMPs, the proteins that *Toxoplasma gondii* secretes into host cells can directly regulate host innate immunity [12-15]. Understanding how and where parasites regulate the IFN-1 response could shed light on alternative modes of IFN-1 production by non-viral pathogens.

Here we show that inflammatory monocytes (IMs), but not neutrophils, produce IFN-β in response to *T. gondii* infection. This difference correlated with the mode of parasite entry into host cells, with phagocytic uptake predominating in IMs and active invasion predominating in neutrophils. We also show that expression of IFN-β by IMs requires phagocytic uptake of parasites as well as signaling through TLR4 and MyD88. Finally, we show that IMs are the major producers of IFN-β in mesenteric lymph nodes following *in vivo* oral infection of mice. Our data reveal a TLR and internalization-dependent pathway in IMs for IFN-β induction to a non-viral pathogen.

RESULTS

TLR dependent IFN-β induction after infection of inflammatory monocytes *in vitro*

To investigate the mechanism of IFN-β induction in response to *T. gondii* infection, we infected freshly isolated bone marrow cells with parasites, and examined IFN-β mRNA levels by qRT-PCR at different times after infection. For these experiments, we used irradiated parasites, which can invade host cells but cannot replicate, in order to avoid host cell death at later time points. We observed an increase in IFN-β mRNA that peaked around 8 hours after infection (Fig. 1A). Thus, *in vitro* infection of bone marrow cells provides a convenient assay to study IFN-β induction in response to *T. gondii* infection.

Separate flow cytometric analysis of bone marrow cells infected *in vitro* with RFP-expressing parasites revealed that the RFP signal was preferentially found within $Ly6C^{high}CD11b^{+}$ cells as well as $Ly6G^{+}CD11b^{+}$ cells (neutrophils) (Fig. 2A). $Ly6C^{high}CD11b^{+}$ cells are rapidly released from the bone marrow in response to infection and give rise to IMs found at sites of infection [16]. For brevity, we refer herein to $Ly6C^{high}CD11b^{+}$ cells from both the resting bone marrow and from infected mice as IMs. IMs have been previously implicated in IFN-1 production in response to certain viruses and bacteria [17-20]. To determine whether IMs or neutrophils contribute significantly to the IFN-β response to *T. gondii*, we enriched bone marrow cells for different cell types prior to infection. Because no single marker distinguishes IMs from other cells, we enriched for IMs and neutrophils using Ly6-B2, or enriched for neutrophils only using Ly6G (Fig. 1B and 1C). Ly6-B2 and Ly6G have been used in combination to distinguish IMs from neutrophils in tissue sections [21]. Both enrichment procedures effectively removed pDCs (Fig. 1B), which are known to be the major producers of IFN-β following viral infection and have also been reported to express IFN-β *in vitro* in response to *T. gondii* [22, 23]. We observe significant induction of IFN-β from Ly6-B2 enriched fractions, but not from neutrophil only (Ly6G-enriched) fractions (Fig. 1C). The level of IFN-β produced by Ly6-B2 enriched bone marrow cells in response to parasites is comparable in magnitude to the response to the TLR3 agonist, polyIC (Fig. 1C). It is noteworthy, however, that the response of unfractionated bone marrow to parasites is considerably higher than the response of Ly6-B2-enriched cells to parasites, indicating that the majority of the response of bone marrow cells to parasites is found in the Ly6-B2 negative population (Fig 1C). We chose to focus on IFN-β production from the IM population because they represent an important population during in vivo *Toxoplasma* infection [24], and because our preliminary in vivo experiments implicated IMs, rather than pDCs in IFN-β production after oral infection (data not shown).

Multiple TLRs have been previously implicated in sensing *T. gondii*, including the sensing of parasite profillin via TLR11 and 12 and parasite glycosylphosphatidylinositols (GPI) 4-anchored proteins via TLR2 and 4 [3, 6]. To examine the role of TLRs in IFN-β production by IMs, we examined responses in bone marrow cells isolated from various mutant mice. Ly6-B2 enriched bone marrow cells from MyD88 knockout mice failed to express IFN-β in response to *T. gondii* infection, consistent with a role for TLR signaling (Fig. 1D). Moreover, production of IFN-β by $Ly6\text{-}B2^{+}$ cells isolated from TLR4 KO or from TLR2x4 double KO mice was reduced to near the levels of the uninfected control samples, whereas

loss of TLR2 led to a more modest reduction that did not reach statistical significance (Fig. 1E). These data suggest that TLR4 is the predominant TLR through which IMs trigger IFN-β production in response to *T. gondii*.

Uptake of parasite material is necessary for IFN-β production by inflammatory monocytes

IFN-1 is induced by intracellular infection and typically involves intracellular detection of PAMPs [25]. Flow cytometry analysis of whole bone marrow infected with red fluorescent protein (RFP)-labeled parasites revealed that a large proportion of IMs contained parasite fluorescence (25-50%) (Fig. 2A), suggesting that IFN-β production by IMs may involve intracellular detection of parasite PAMPs. To further investigate this possibility, we infected bone marrow cells with RFP expressing parasites, fractionated Ly6-B2$^+$ cells into parasite containing (RFP$^+$) and non-containing (RFP$^-$) populations and compared IFN-β expression by qRT-PCR analysis. IFN-β expression was limited to the RFP$^+$ Ly6-B2$^+$ cells (Fig. 2B and 2C), suggesting that the production of IFN-β by IMs occurs via intracellular recognition of *T. gondii* PAMPs.

IMs containing fluorescent parasites may have taken up parasites by phagocytosis or may have been actively invaded by the parasites. To examine the mode of parasite internalization by IMs, we infected bone morrow cells, sorted IMs (Ly6-B2$^+$Ly6G$^-$) by FACS, and performed immunofluorescence microscopy using antibodies to a parasite protein, GRA6, which accumulates in the parasitophorous vacuole of invaded cells. We find that ~70% (282 out of 413) of RFP$^+$ IMs show GRA6 staining adjacent to RFP parasites, suggesting productive invasion by the parasite. The remaining ~30% (131 out of 413) showed no detectable GRA6 staining and a more amorphous RFP signal suggestive of phagocytosis or parasite destruction by the host cell (Fig. 3A). Thus, the RFP signal in IMs likely reflects both active invasion by the parasites and phagocytic uptake of parasites by the IMs.

To separate IMs that were invaded from those that phagocytosed parasites, we took advantage of a genetically engineered RFP-labeled parasite strain that injects Cre protein into host cells during active invasion, driving expression of GFP in cells from Cre-regulated GFP reporter mice [26, 27]. Host cells harboring parasites due to active invasion (“successfully infected”) can be identified by co-expression of GFP and RFP. Host cells that have taken up parasites by phagocytosis, which does not allow Cre access to the host nucleus, will be contained within the RFP only fraction (Fig. 3B). In addition, since it takes several hours for GFP expression to be detectable following Cre injection into host cells, recently invaded cells will also be RFP$^+$GFP$^-$. Host cells that were injected with parasite effectors but not infected, as well as those that were invaded but subsequently killed and degraded the parasites (“injected/uninfected”) express GFP but not RFP. Eight hours after infection, Ly6-B2$^+$ cells were FACS-sorted based on RFP and GFP levels, and IFN-β expression was measured by qRT-PCR (Fig. 3C). IFN-β was predominantly produced by GFP$^-$RFP$^+$ (phagocytosis) cells, with only background IFN-β levels in the GFP$^+$RFP$^+$ (successfully infected) population, indicating that active invasion of IMs does not trigger IFN-β induction. Interestingly, the injected/uninfected subpopulation (GFP$^+$RFP$^-$) had IFN-β levels below uninfected, suggesting the ability of parasite effectors to down modulate IFN-β expression, as had been previously suggested [28]. It is also noteworthy that the ratio of GFP$^+$RFP$^+$

(successfully infected) to $GFP^{-}RFP^{+}$ (phagocytosed) IMs was ~0.7, in contrast to neutrophils where the ratio was ~1.7 (Fig. 3D and 3E). This indicates that neutrophils are a better target for successful invasion compared to IMs, which may in part account for their failure to produce IFN-β in response to *T. gondii* (Fig. 3E).

To further explore the impact of invasion versus phagocytosis on IFN-β induction, we examined responses to heat-killed parasites, which can be phagocytosed but cannot invade. Interestingly, the response to heat-killed parasites was greater than the response to live parasites, particularly at higher ratios of parasites to host cells, while increasing numbers of live parasites appeared to inhibit IFN-β induction (Fig. 3F). These data, together with an earlier report [28], indicate that active invasion does not trigger IFN-β induction, but rather inhibits the response.

To further test whether phagocytosis is required for IFN-β induction, we treated cells with Latrunculin A, a drug that prevents phagocytosis through actin depolymerization [29]. Treatment with Latrunculin A led to reduced uptake of parasites, as indicated by a drop in RFP fluorescence, particularly in IMs (Fig 3G). Latrunculin A treatment also led to a reduction in IFN-β expression to background levels (Fig. 3G). To control for cell viability, we stimulated drug treated cells with LPS (TLR4 ligand) and Pam_3 (TLR2 ligand), which are known to induce TNF-α though the activation of TLRs on the cell surface. We confirmed that TNF-α production in response to LPS (TLR4 ligand) and Pam_3 (TLR2 ligand) was unaffected by Latrunculin A treatment (Fig. 3H). Interestingly, TNF-α production in response to heat-killed parasites was also inhibited by Latrunculin A, suggesting that induction of TNF-α also requires parasite internalization (Fig. 3H).

Inflammatory monocytes produce IFN-β after oral *T. gondii* infection

We next sought to extend our *in vitro* observations to an *in vivo* oral infection setting. We orally infected mice with *Toxoplasma* cysts, harvested the gut-draining mesenteric lymph nodes (MLNs) at various times post-infection, and analyzed IFN-β expression by qRT-PCR. Expression of IFN-β was consistently elevated at days 4-7 post-infection, although there was considerable mouse-to-mouse variation in the level of induction (Fig 4A). We then asked whether IMs contributed significantly to IFN-β induction *in vivo*. We used a cell depletion approach to address this question, which provided a more a robust assay with limited cell numbers. We compared samples depleted of $Ly6\text{-}B2^{+}$ cells (IMs and neutrophils, ~3% of starting MLN cells) or $Ly6G^{+}$ cells (neutrophils only, ~0.25% of starting MLN cells). As a control, we also analyzed the starting samples and samples depleted of T cells using antibodies to CD3 (~40% of starting MLN cells). Notably, depletion of both neutrophils and IMs led to a 2-fold decrease of IFN-β, whereas depletion of neutrophils alone had no significant effect (Fig. 4B-D). It is also noteworthy that depletion of T cells, which led to a proportional increase of IMs in the population, led to a 2.5 fold increase of IFN-β expression. Together these data suggest that IMs contribute significantly to the IFN-β expression by MLN cells after oral *T. gondii* infection. We also found that mice lacking the TLR adaptor MyD88 displayed significantly reduced IFN-β induction in MLNs 5 days following oral infection (Fig. 4E). The lack of requirement for TLR7 or TLR9 (Fig. 4F) is consistent with a lack of involvement of pDCs in this response. Taken together these data

indicate that IMs produce IFN-β in a Myd88-dependent manner following *T. gondii* infection *both in vivo* and *in vitro*.

Finally, to determine the consequences of IFN-1 induction during *T. gondii* infection, we infected mice lacking the receptor for IFN-1 (IFNAR KO) orally with tissue cysts and monitored parasite load in the gut draining mesenteric lymph node at 5 days post infection. We observed an increase in parasite load in mutant compared to wild type (WT) C57Bl/6 mice (Fig. 5A), which correlated with a small, but statistically significant, decrease in survival (Fig 5B). Female mice are known to be more susceptible than male mice to *Toxoplasma* infection, and thus we examined the data separately for female and male mice. Interestingly, the increase in parasite load in INFAR KO mice was more significant when only female mice were compared (Fig 5A), whereas the survival difference in IFNAR KO mice was more pronounced when only male mice were considered (Fig 5B). These results suggest that IFN-1 induced upon oral infection by *T. gondii* plays a modest protective role, resulting in decreased parasite load and increased survival in WT compared to IFNAR KO mice.

DISCUSSION

IFN-1 induction in response to viral infection has been extensively studied, but the mechanism of induction during parasitic infection is less well understood. For *Toxoplasma gondii*, we lack key information about the host innate immune sensors, the specialized cell types, and intracellular signaling compartments involved. Here we show that IMs, but not neutrophils, produce IFN-β in response to *T. gondii*. We also show that IFN-β production requires phagocytic uptake of the parasite by IMs and is reduced in IMs lacking TLR4 or MyD88. Finally we show that IMs are the major source of IFN-β in the gut-draining MLNs after oral infection. Our data identify TLR and phagocytosis dependent detection of parasite PAMPs by IMs and shed light on the mechanism of IFN-β production during infection by a non-viral pathogen.

Toxoplasma gondii can stimulate innate immunity via multiple TLRs, including TLR11 and 12 detection of the parasite protein profillin [3, 4, 30], and TLR2 and 4 detection of parasite GPIs (14). Profillin can induce IL12 expression by DCs via TLR11 and TLR12, and interferon- production by pDCs *in vitro* [3-5, 30]. In addition, *in vitro* exposure of macrophages to parasite GPIs triggers TNF-α via TLRs 2 and 4 [6]. Here we show that a distinct cell type, the inflammatory monocyte, produces IFN-β in a TLR4 and MyD88 dependent fashion. Altogether, these results highlight how specificity in innate immune responses can be generated by different TLRs acting in specialized cell types, thus allowing for distinct host responses to be triggered by a single pathogen.

Interestingly, production of IFN-β by IMs requires uptake of the parasite into the host cell, reminiscent of the requirement for TLR2 internalization for IFN-β induction by certain viruses [31]. Internalization may be necessary to deliver TLR2 and TLR4 to an intracellular compartment that is permissive for IFN-1 induction. This would be analogous to the requirement for endosomal trafficking of TLR4 by CD14 and LPS [32], and the AP3-dependent transport of TLR9 and CpG ligands to a $LAMP2^+$ lysosome related organelle [8].

Thus, our data fit with an emerging theme in which the initial encounter between TLR and ligand is sufficient to trigger inflammatory cytokine production, whereas an additional ligand-dependent transport step is required for IFN-1 production.

In addition to allowing for intracellular triggering of TLRs, uptake of parasites by host IMs may also be necessary to process parasite PAMPs for recognition by TLRs. In fact, it has been previously shown that TLR2 can be triggered by the lipid and glycan moiety of parasite GPIs, but not intact GPI, leading to the suggestion that processing of GPI by macrophage phospholipase occurs prior to TLR recognition [33]. A requirement for intracellular processing of parasite PAMPs could also help to explain our observation that endocytosis is required for both TNF-α and IFN-β production by IMs in response to heat-killed parasites.

IMs play a key role in host protection against oral infection by *T. gondii* [24], although the precise mechanism of protection is unknown. Our data suggest that part of the protective function of IMs may lie in their ability to detect the parasites early during infection and to elaborate cytokines, such as IFN-β, to orchestrate subsequent immune responses.

Toxoplasma is highly adapted to grow within its mammalian host and can actively manipulate host immune responses via a variety of secreted effectors [34]. In this regard, it is intriguing that live parasites, which can actively invade host cells, triggered a weaker IFN-β response compared to heat-killed parasites, as reported here and in an independent study [28]. Moreover, neutrophils, which preferentially harbor live parasites, failed to produce IFN-β in response to *T. gondii*. These observations suggest that live *Toxoplasma* parasites may actively suppress host IFN-β production consistent with a previous report [28]. Along these same lines, while TNF-α induction by parasite PAMPs can be detected in some studies [6], other studies reveal the inhibition of TNF-α by active parasite invasion [35]. Thus, during *Toxoplasma* infection, the overall innate immune response of the mammalian host triggered by detection of parasite PAMPs by innate immune sensors is counterbalanced by active suppression by the parasites. In this regard, it is interesting to consider that the ratio of live to dead parasites encountered by host cells in different infection settings could be a crucial factor in determining whether parasite suppression of host immunity wins out over parasite detection by the host immune system.

Methods

Mice

C57Bl/6, MyD88 KO and Cre-regulated GFP reporter (Rosa26-Cre) [27] mice were purchased from Jackson or were bred in-house and maintained under specific pathogen-free conditions at the AALAC approved Life Science Addition animal facility at the University of California, Berkeley. In brief, the Cre-reporter mice have been engineered with a green fluorescent protein gene (ZsGreen) downstream of a transcriptional stop codon that is flanked by *loxP* sites knocked into the Rosa26 locus. Thus, only after Cre-mediated recombination will the cells express GFP. All experiments were approved by the Animal Care and Use Committee at UC Berkeley. IFNAR KO mice were a gift from Dr. D. Portnoy (UC Berkeley). The LysM-GFP reporter mice were a gift from Dr. T. Graf (Albert Einstein College of Medicine, Bronx, NY) and have been previously described [36]. In experiments

using TLR2/4 KO mice, both the mutant and C57Bl/6 control mice carried a functional nramp1 allele (G169) 37. For the majority of *in vivo* experiments, KO mice were co-housed with WT control mice. Since some antibiotics can inhibit *Toxoplasma gondii* growth, we placed all mice on drinking water without antibiotics at least one week before oral infection.

T. gondii infections

Type II Prugniaud parasites engineered to express RFP and ovalbumin were maintained, purified, and used for oral infection as described previously [38]. Mice were infected with 30-50 cysts by oral gavage. For the *in vitro* experiments, parasites were irradiated with 14000 rad or heat-killed for 10min in a 56°C waterbath. Parasite cultures were regularly screened for mycoplasma contamination and confirmed to be negative. To identify actively invaded cells, bone marrow cells from mice bearing a Cre-regulated GFP reporter were infected with parasites engineered to secrete Cre upon invasion of host cells. To generate this parasite strain, the above described parental Type II Prugniaud parasites engineered to express RFP and Ova and which lack the endogenous gene for hypoxanthine xanthine guanine phosphoribosyl transferase (HPT) were electroporated with a previously described linearized vector (*ptoxofilin-Cre*) [26], which expresses the selectable *HPT* marker and the epitope tagged rhoptry protein toxofilin fused to Cre recombinase. As previously described, the parasites were then subjected to several rounds of selection for the expression of HPT using media containing 25 μg/ml mycophenolic acid and 50 μg/ml xanthine before being cloned by limiting dilution [39]. To verify secretion of a functional toxofilin:Cre fusion protein, single clones that were HPT^+ were then tested for efficacy in causing Cre-mediated recombination in a Cre-reporter cell line [26].

Tissue digestion and flow cytometry

All infected and uninfected tissues were dissociated by collagenase digestion as described previously [40]. Cell suspensions were stained and analyzed by flow cytometry. The following antibodies were used for cell surface staining: anti-CD11b (clone M1/70), anti-CD11c (clone N418), anti-CD3 (145-2C11), anti-Ly6C (HK1.4), anti-MHCII (M5/114.15.2), anti-CD19 (ebio1D3), anti-NK1.1 (PK136), anti-siglecH (ebio440c), anti-B220 (RA3-6B2), anti-CD4 (GK.5), anti-CD8 (53-6.7) and anti-CD69 (H1.2F3) were purchased from eBioscience, anti-Ly6G (1A8) was obtained from BD Pharmingen, anti-Ly6-B2 antibody (7/4) from AbD Serotec, and CCR2 (475301) from R&D Systems. For intracellular staining: anti-iNOS antibody was purchased from Millipore, and anti-TNF-α (MP6-XT22) was purchased from BD Pharmingen. Cell suspensions from collagenase-digested tissue were stained for cell surface markers and permeabilized using the BD Cytofix/Cytoperm Kit (BD Pharmingen). For detection of intracellular TNF-α, cells were also treated *ex vivo* with GolgiPlug (BD Pharmingen) for 6 h at 37°C in complete RPMI medium prior to cell surface staining and stained according to the manufacturers instructions. Acquisitions were performed with a BD LSRII, and data were analyzed with the FlowJo software.

Real-time PCR

Cell suspensions from collagenase-digested tissue were lysed in Trizol (Invitrogen), and mRNA was isolated using the Qiagen RNeasy Mini Kit (Qiagen). A total of 1 to 2 μg of

mRNA was used for reverse transcription using the QuantiTect Reverse Transcription Kit (Qiagen). cDNA was amplified using 2x SYBR green mix (AB Applied Biosystems) on a 7300 real-time PCR system from AB Applied Biosystems. IFN-β expression was normalized to GAPDH and $\Delta\Delta C_T$ analysis was used to determine relative expression among samples. The following primers were used: IFN-β: forward GTT ACA CTG CCT TTG CCA TCC AAG and reverse ACT GTC TGC TGG TGG AGT TCA TCC; GAPDH: forward TGG CAA AGT GGA GAT TGT TGC C and reverse AAG ATG GTG ATG GGC TTC CCG. For some experiments, we present IFN-β expression in KO mice normalized to the average of IFN-β expression in infected WT mice analyzed on the same day. We occasionally performed experiments in which the *in vitro* response of all cell populations, including wild type Ly6-B2-enriched bone marrow cells was weak (<2.5 fold). We suspect that this was due to variation in the state of irradiated parasites, perhaps related to the ability of the parasites to be phagocytosed versus their ability to invade the host cells. To facilitate comparisons of wild type versus mutant or manipulated samples, we excluded whole experiments in which no Toxoplasma treated samples showed induction of 2.5 –fold or greater compared to uninfected. As an alternative to real-time PCR, we attempted to use the previously described fluorescent IFN-β reporter mice [41]. However overlap from the RFP signal of the parasites complicated the detection of this already weak fluorescent signal, rendering this reporter unsuitable for this study.

Ex vivo depletion of cell populations

MLNs from orally infected WT mice were collagenase digested and cell populations were depleted as indicated using EasySep Biotin Positive Selection Kit (Stemcell Technologies) according to the manufacturers instructions for cell depletion.

Preparation and Enrichment of cell populations and *in vitro* infection

Bone marrow cells were isolated from adult mouse leg bones by flushing the interior with a syringe filled with media, and filtering through nylon mesh to generate a single cell suspension. $Ly6G^+$ and $Ly6\text{-}B2^+$ cells were enriched from bone marrow cells of WT and the variously engineered mice using the EasySep Biotin Positive Selection Kit according to the manufacturers instructions (Stemcell Technologies.) Pre-, $Ly6G^+$- and $Ly6\text{-}B2^+$-enriched cells (2.5×10^6 cells per well in a 12 well tissue culture plate) were infected for 8hrs with irradiated parasites (MOI = 1-2). To ensure that there was no fibroblast carry-over from the parasite maintenance cultures, fibroblast cultures were harvested under parasite preparation conditions and incubated with uninfected control cells. In the figures, this condition was referred to as the uninfected starting population.

Latrunculin A treatment

Pre-, $Ly6G^+$- and $Ly6\text{-}B2^+$-enriched cells (2.5×10^6) were treated with 0.1 μg/ml Latrunculin A for 30-45min at 37°C. Treated and untreated cells were stimulated for 8hrs with heat-killed parasites at a ratio of 2 parasites / cell. For intracellular TNF-α detection, bone marrow cells were treated with 0.1 μg/ml Latrunculin A (Invitrogen) for 30-45min prior to stimulation with heat-killed parasites as above, LPS (1 μg/ml) or Pam_3 (1 μg/ml). 30min

after stimulation, GolgiPlug was added for an additional 7hrs, and intracellular TNF-α was detected as described above.

Fluorescence-activated cell sorting (FACS)

WT bone marrow cells were infected (MOI=1-2) with RFP expressing live parasites for 8hrs and stained with anti-CD11b, Ly6G and Ly6-B2 antibodies. RFP positive and RFP negative Ly6-B2^{+}CD11b^{+} cells were sorted using a Moflo cell sorter.

Immunofluorescence Microscopy

WT bone marrow cells were infected with live parasites for 8hrs and 2×10^{5} Ly6-B2^{+}Ly6G^{-} bone marrow cells were sorted using FACS. FACS-sorted cells were spun onto slides and stained for GRA6 as described previously [42]. Images were taken using a Nikon TE2000 inverted microscope with 40X/1.3 Nikon oil objectives. Images were acquired using NIS Elements AR software and processed using Imaris software.

Statistical Analysis

Values are expressed as mean ± standard error (SEM). Statistical significance was calculated using a one-way ANOVA and Tukey post hoc test unless otherwise indicated. Differences were considered significant at $p < 0.05$. To calculate the statistics for figures 4D, 4E and 4F, the values were first transformed using the natural logarithms due to the differences in the standard deviation of each group.

Acknowledgements

The authors would like to thank Hector Nolla and Alma Valeros for cell sorting (UC Berkeley CRL Flow Cytometry Facility), Boris Striepen for the engineered RFP-expressing parasites, members of the Robey, Barton, and Boothroyd labs for helpful suggestions and reagents. This work was funded by NIH grants R01 AI065537 and R01 AI093132 (to E.A.R.), PO1 AI065831 (to E.A.R.), RO1 AI21423 (to J.C.B.), and KO8 NS 065116 (to A.A.K.), and Wellcome Trust grant WT085494 (to J.L.C).

References

1. Scanga CA, Aliberti J, Jankovic D, Tilloy F, Bennouna S, Denkers EY, et al. Cutting edge: MyD88 is required for resistance to Toxoplasma gondii infection and regulates parasite-induced IL-12 production by dendritic cells. J Immunol. 2002; 168:5997–6001. [PubMed: 12055206]
2. Sukhumavasi W, Egan CE, Warren AL, Taylor GA, Fox BA, Bzik DJ, et al. TLR adaptor MyD88 is essential for pathogen control during oral toxoplasma gondii infection but not adaptive immunity induced by a vaccine strain of the parasite. J Immunol. 2008; 181:3464–73. [PubMed: 18714019]
3. Koblansky AA, Jankovic D, Oh H, Hieny S, Sungnak W, Mathur R, et al. Recognition of profilin by Toll-like receptor 12 is critical for host resistance to Toxoplasma gondii. Immunity. 2013; 38:119–30. [PubMed: 23246311]
4. Yarovinsky F, Zhang D, Andersen JF, Bannenberg GL, Serhan CN, Hayden MS, et al. TLR11 activation of dendritic cells by a protozoan profilin-like protein. Science. 2005; 308:1626–9. [PubMed: 15860593]
5. Mashayekhi M, Sandau MM, Dunay IR, Frickel EM, Khan A, Goldszmid RS, et al. CD8alpha(+) dendritic cells are the critical source of interleukin-12 that controls acute infection by Toxoplasma gondii tachyzoites. Immunity. 2011; 35:249–59. [PubMed: 21867928]
6. Debierre-Grockiego F, Campos MA, Azzouz N, Schmidt J, Bieker U, Resende MG, et al. Activation of TLR2 and TLR4 by glycosylphosphatidylinositols derived from Toxoplasma gondii. J Immunol. 2007; 179:1129–37. [PubMed: 17617606]

7. Debierre-Grockiego F, Azzouz N, Schmidt J, Dubremetz JF, Geyer H, Geyer R, et al. Roles of glycosylphosphatidylinositols of Toxoplasma gondii. Induction of tumor necrosis factor-alpha production in macrophages. J Biol Chem. 2003; 278:32987–93. [PubMed: 12815041]
8. Sasai M, Linehan MM, Iwasaki A. Bifurcation of Toll-like receptor 9 signaling by adaptor protein 3. Science. 2010; 329:1530–4. [PubMed: 20847273]
9. Honda K, Yanai H, Negishi H, Asagiri M, Sato M, Mizutani T, et al. IRF-7 is the master regulator of type-I interferon-dependent immune responses. Nature. 2005; 434:772–7. [PubMed: 15800576]
10. Blasius AL, Beutler B. Intracellular toll-like receptors. Immunity. 2010; 32:305–15. [PubMed: 20346772]
11. Barton GM, Kagan JC. A cell biological view of Toll-like receptor function: regulation through compartmentalization. Nat Rev Immunol. 2009; 9:535–42. [PubMed: 19556980]
12. Rosowski EE, Lu D, Julien L, Rodda L, Gaiser RA, Jensen KD, et al. Strain-specific activation of the NF-kappaB pathway by GRA15, a novel Toxoplasma gondii dense granule protein. J Exp Med. 2011; 208:195–212. [PubMed: 21199955]
13. Yamamoto M, Standley DM, Takashima S, Saiga H, Okuyama M, Kayama H, et al. A single polymorphic amino acid on Toxoplasma gondii kinase ROP16 determines the direct and strain-specific activation of Stat3. J Exp Med. 2009; 206:2747–60.
14. Saeij JP, Coller S, Boyle JP, Jerome ME, White MW, Boothroyd JC. Toxoplasma co-opts host gene expression by injection of a polymorphic kinase homologue. Nature. 2007; 445:324–7.
15. Ong YC, Reese ML, Boothroyd JC. Toxoplasma rhoptry protein 16 (ROP16) subverts host function by direct tyrosine phosphorylation of STAT6. J Biol Chem. 2010; 285:28731–40. [PubMed: 20624917]
16. Shi C, Pamer EG. Monocyte recruitment during infection and inflammation. Nat Rev Immunol. 2011; 11:762–74. [PubMed: 21984070]
17. Fitzgerald-Bocarsly P, Dai J, Singh S. Plasmacytoid dendritic cells and type I IFN: 50 years of convergent history. Cytokine Growth Factor Rev. 2008; 19:3–19. [PubMed: 18248767]
18. Burdette DL, Monroe KM, Sotelo-Troha K, Iwig JS, Eckert B, Hyodo M, et al. STING is a direct innate immune sensor of cyclic di-GMP. Nature. 2011; 478:515–8. [PubMed: 21947006]
19. Stetson DB, Medzhitov R. Recognition of cytosolic DNA activates an IRF3-dependent innate immune response. Immunity. 2006; 24:93–103. [PubMed: 16413926]
20. Woodward JJ, Iavarone AT, Portnoy DA. c-di-AMP secreted by intracellular Listeria monocytogenes activates a host type I interferon response. Science. 2010; 328:1703–5. [PubMed: 20508090]
21. Kang SJ, Liang HE, Reizis B, Locksley RM. Regulation of hierarchical clustering and activation of innate immune cells by dendritic cells. Immunity. 2008; 29:819–33. [PubMed: 19006696]
22. Pepper M, Dzierszinski F, Wilson E, Tait E, Fang Q, Yarovinsky F, et al. Plasmacytoid dendritic cells are activated by Toxoplasma gondii to present antigen and produce cytokines. J Immunol. 2008; 180:6229–36. [PubMed: 18424745]
23. Gilliet M, Cao W, Liu YJ. Plasmacytoid dendritic cells: sensing nucleic acids in viral infection and autoimmune diseases. Nat Rev Immunol. 2008; 8:594–606. [PubMed: 18641647]
24. Dunay IR, Damatta RA, Fux B, Presti R, Greco S, Colonna M, et al. Gr1(+) inflammatory monocytes are required for mucosal resistance to the pathogen Toxoplasma gondii. Immunity. 2008; 29:306–17. [PubMed: 18691912]
25. Takeuchi O, Akira S. Innate immunity to virus infection. Immunol Rev. 2009; 227:75–86. [PubMed: 19120477]
26. Koshy AA, Fouts AE, Lodoen MB, Alkan O, Blau HM, Boothroyd JC. Toxoplasma secreting Cre recombinase for analysis of host-parasite interactions. Nat Methods. 2010; 7:307–9. [PubMed: 20208532]
27. Madisen L, Zwingman TA, Sunkin SM, Oh SW, Zariwala HA, Gu H, et al. A robust and high-throughput Cre reporting and characterization system for the whole mouse brain. Nat Neurosci. 2010; 13:133–40. [PubMed: 20023653]
28. Beiting DP, Peixoto L, Akopyants NS, Beverley SM, Wherry EJ, Christian DA, et al. Differential induction of TLR3-dependent innate immune signaling by closely related parasite species. PLoS One. 2014; 9:e88398. [PubMed: 24505488]

29. Oliveira CA, Kashman Y, Mantovani B. Effects of latrunculin A on immunological phagocytosis and macrophage spreading-associated changes in the F-actin/G-actin content of the cells. Chem Biol Interact. 1996; 100:141–53. [PubMed: 8646787]
30. Andrade WA, Souza MdC, Ramos-Martinez E, Nagpal K, Dutra MS, Melo MB, et al. Combined Action of Nucleic Acid-Sensing Toll-like Receptors and TLR11/TLR12 Heterodimers Imparts Resistance to Toxoplasma gondii in Mice. Cell host & microbe. 2013; 13:42–53. [PubMed: 23290966]
31. Barbalat R, Lau L, Locksley RM, Barton GM. Toll-like receptor 2 on inflammatory monocytes induces type I interferon in response to viral but not bacterial ligands. Nat Immunol. 2009; 10:1200–7. [PubMed: 19801985]
32. Zanoni I, Ostuni R, Marek LR, Barresi S, Barbalat R, Barton GM, et al. CD14 Controls the LPS-Induced Endocytosis of Toll-like Receptor 4. Cell. 2011; 147:868–880. [PubMed: 22078883]
33. Debierre-Grockiego F, Niehus S, Coddeville B, Elass E, Poirier F, Weingart R, et al. Binding of Toxoplasma gondii glycosylphosphatidylinositols to galectin-3 is required for their recognition by macrophages. J Biol Chem. 2010; 285:32744–50. [PubMed: 20729207]
34. Lim DC, Cooke BM, Doerig C, Saeij JP. Toxoplasma and Plasmodium protein kinases: roles in invasion and host cell remodelling. Int J Parasitol. 2012; 42:21–32. [PubMed: 22154850]
35. Denkers EY, Butcher BA, Del Rio L, Kim L. Manipulation of mitogen-activated protein kinase/nuclear factor-kappaB-signaling cascades during intracellular Toxoplasma gondii infection. Immunol Rev. 2004; 201:191–205. [PubMed: 15361242]
36. Faust N, Varas F, Kelly LM, Heck S, Graf T. Insertion of enhanced green fluorescent protein into the lysozyme gene creates mice with green fluorescent granulocytes and macrophages. Blood. 2000; 96:719–26. [PubMed: 10887140]
37. Arpaia N, Godec J, Lau L, Sivick KE, McLaughlin LM, Jones MB, et al. TLR signaling is required for Salmonella typhimurium virulence. Cell. 2011; 144:675–88. [PubMed: 21376231]
38. Chtanova T, Schaeffer M, Han SJ, van Dooren GG, Nollmann M, Herzmark P, et al. Dynamics of neutrophil migration in lymph nodes during infection. Immunity. 2008; 29:487–96. [PubMed: 18718768]
39. Donald RG, Carter D, Ullman B, Roos DS. Insertional tagging, cloning, and expression of the Toxoplasma gondii hypoxanthine xanthine-guanine phosphoribosyltransferase gene. Use as a selectable marker for stable transformation. J Biol Chem. 1996; 271:14010–9. [PubMed: 8662859]
40. Coombes JL, Han S-J, van†Rooijen N, Raulet DH, Robey EA. Infection-Induced Regulation of Natural Killer Cells by Macrophages and Collagen at the Lymph Node Subcapsular Sinus. Cell Reports. 2012; 2:124–135. [PubMed: 22840403]
41. Scheu S, Dresing P, Locksley RM. Visualization of IFNbeta production by plasmacytoid versus conventional dendritic cells under specific stimulation conditions in vivo. Proc Natl Acad Sci U S A. 2008; 105:20416–21. [PubMed: 19088190]
42. Chtanova T, Han SJ, Schaeffer M, van Dooren GG, Herzmark P, Striepen B, et al. Dynamics of T cell, antigen-presenting cell, and pathogen interactions during recall responses in the lymph node. Immunity. 2009; 31:342–55. [PubMed: 19699173]

Europe PMC Funders Author Manuscripts

Europe PMC Funders Author Manuscripts

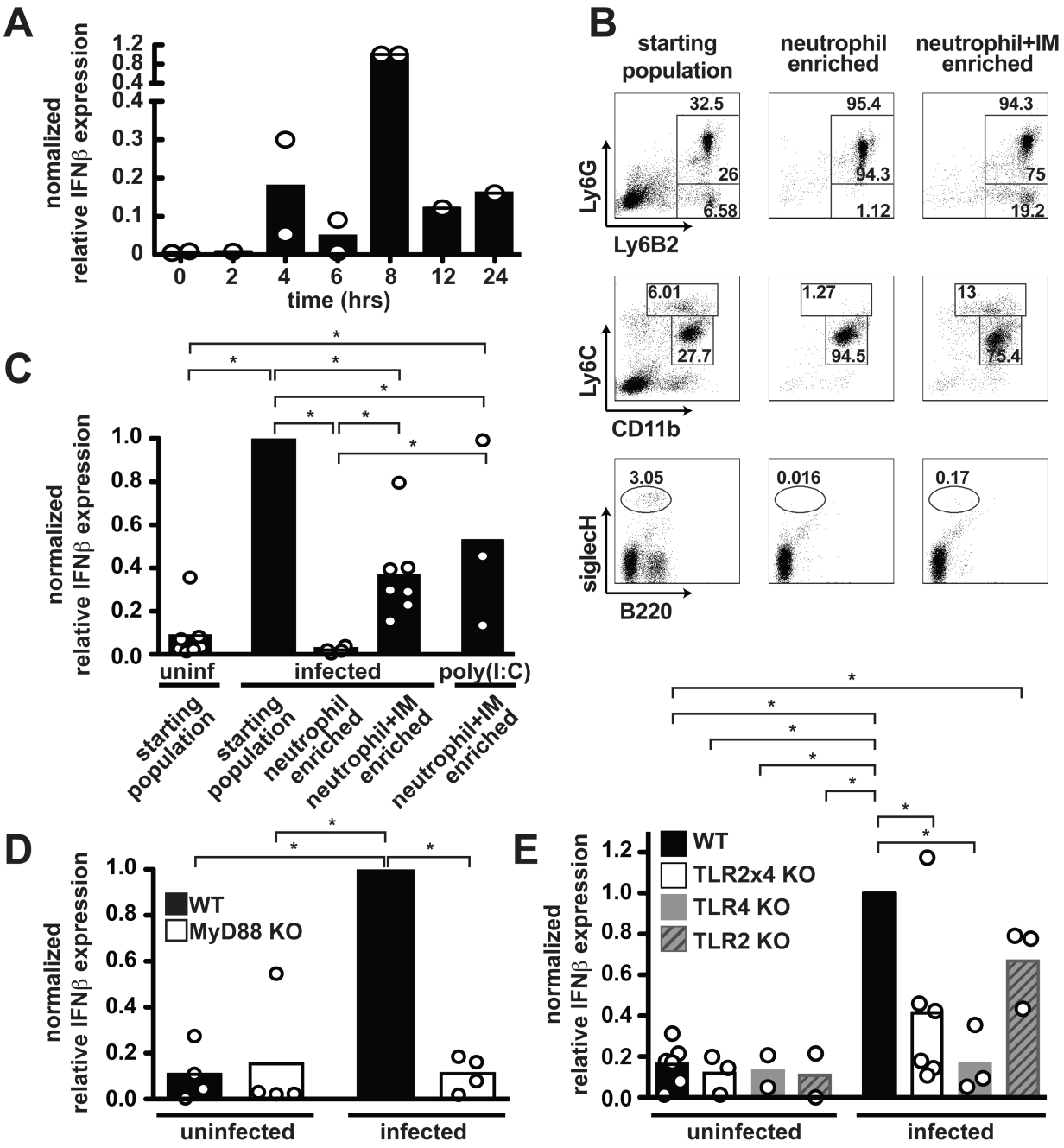

Figure 1. TLR-dependent production of IFN-β by inflammatory monocytes after *T. gondii* infection *in vitro*

(A) bone marrow cells isolated from WT mice were infected *in vitro* with irradiated parasites (MOI=1) and relative IFN-β expression levels at indicated time points were measured by qRT-PCR and normalized to GAPDH in each sample. This experiment was performed twice with similar results and compiled data from both experiments are shown. **(B and C)** bone marrow cells were isolated from WT mice and enriched for $Ly6G^+$ (neutrophils) and $Ly6\text{-}B2^+$ (neutrophils and IMs) cells. Starting population and enriched

Europe PMC Funders Author Manuscripts

populations were infected *in vitro* for 8hrs with irradiated parasites. **(B)** Plots show proportion of $Ly6G^{+}Ly6\text{-}B2^{+}$ and $Ly6G^{-}Ly6\text{-}B2^{+}$ cells (top), $Ly6C^{+}CD11b^{+}$ (middle) and $siglecH^{+}B220^{int}$ (bottom) in non-enriched and enriched samples. **(C)** Relative expression of IFN-β in uninfected and infected starting population and enriched samples of WT bone marrow cells are demonstrated. PolyIC treatment of Ly6-B2 enriched population is shown for comparison. Relative IFN-β expression was measured by qRT-PCR and normalized to GAPDH. IFN-β expression in enriched populations is shown relative to starting population (value = 1). The experiment was performed 7 times with similar results and compiled data from all experiments are shown. Three of the experimental replicates also included a polyIC treated neutrophil + IM enriched sample. Each dot represents value from an individual experiment. ($p=7.19\times10^{-9}$, F=30.32) **(D and E)** Bone marrow cells were isolated from WT and the indicated KO mice and enriched for $Ly6\text{-}B2^{+}$ (neutrophils and IMs) cells. Enriched $Ly6\text{-}B2^{+}$ cells were infected *in vitro* for 8hrs with irradiated parasites. Relative IFN-β expression was measured by qRT-PCR and normalized to GAPDH in each sample. IFN-β expression in mutant samples is shown relative to the IFN-β expression of the WT infected $Ly6\text{-}B2^{+}$ (value=1). Values for uninfected mutant and WT starting populations are shown for comparison. Each dot represents value from an individual experiment. **(D)** Combined data of 4 independent experiments are shown, and each dot represents an individual mouse. ($p=3.34\times10^{-6}$, F=34.85). **(E)** Combined data from 6 independent experiments are shown, and each dot represents an individual mouse. ($p=5.72\times10^{-6}$, F=10.78). Asterisks indicate pairs of values that are statistically different based on a post hoc Tukey test.

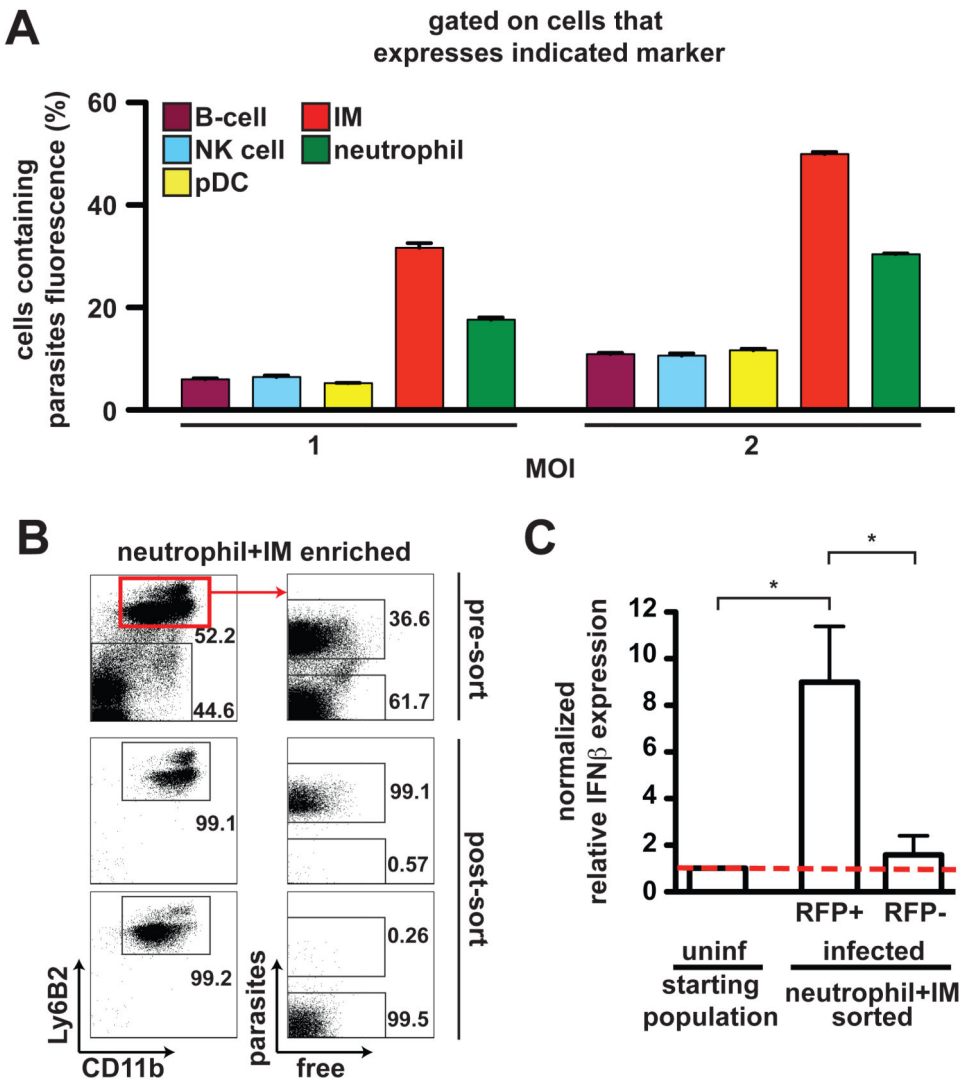

Figure 2. Intracellular detection of parasites triggers IFN-β production by inflammatory monocytes

(A) Bone marrow cells from wild type mice were infected with live RFP+ parasites for 8hrs and then analyzed by flow cytometry. Graph shows proportion of indicated cell population that contains RFP. Experiment was performed twice with similar results and data from a representative experiment is shown. Average values of experimental triplicates are shown. **(B-C)** bone marrow cells were infected *in vitro* for 8hrs with live RFP^+ parasites, Ly6-$B2^+$ cells were sorted for RFP^+ and RFP^- using fluorescence activated cell sorting (FACS), and IFN-β expression was examined by qRT-PCR. Representative flow cytometry plots are shown in **(B)**, and IFN-β expression is shown in **(C)**. IFN-β expression relative to the IFN-β expression of uninfected control sample is shown. Combined data from 4 independent experiments ($p=2.309\times10^{-3}$, $F=12.84$). Asterisks indicate pairs of values that are statistically different based on a post hoc Tukey test.

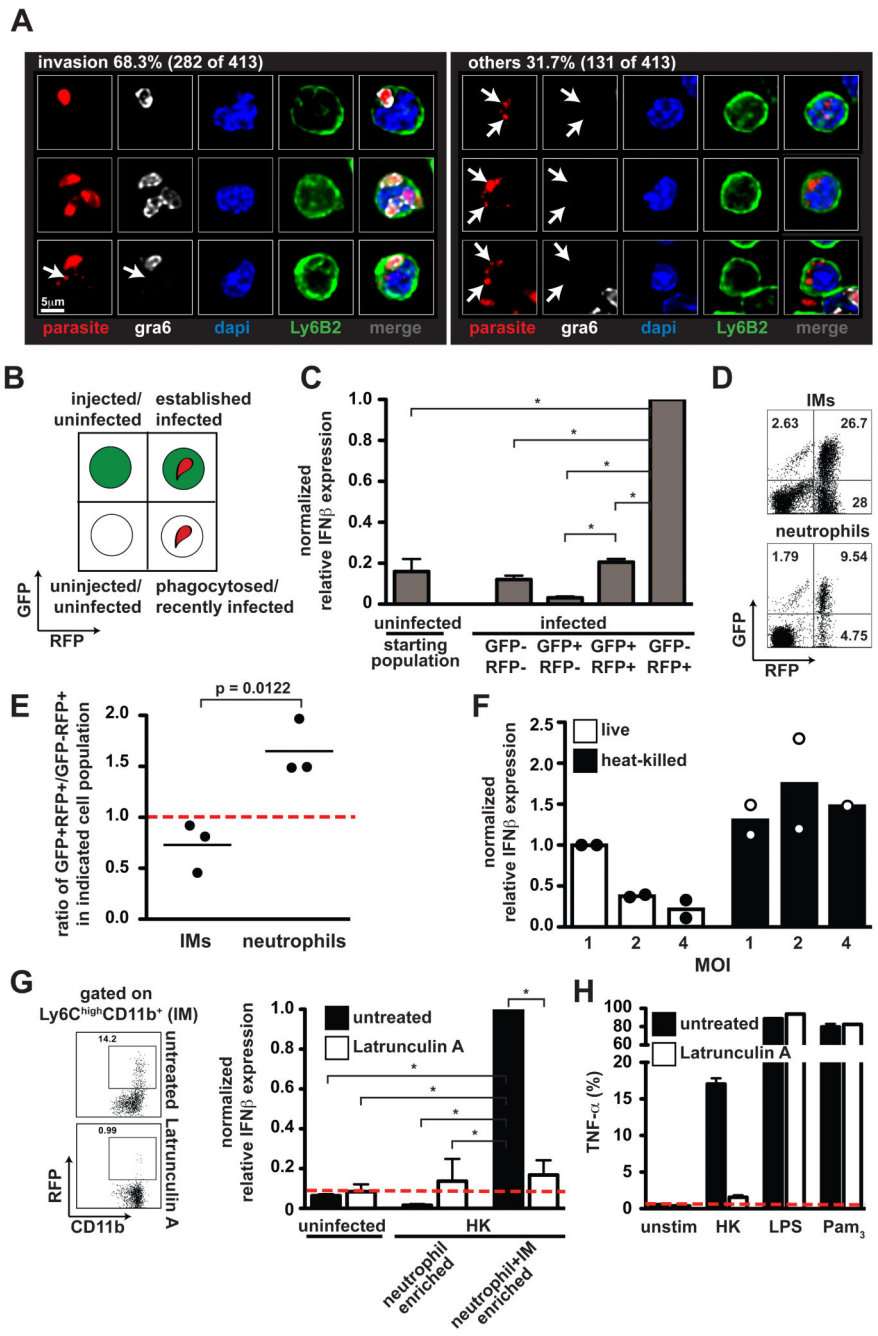

Figure 3. Phagocytosis is necessary for IFN-β production by inflammatory monocytes

(A) Bone marrow cells were infected *in vitro* for 8hrs with live RFP$^+$ parasites and Ly6-B2$^+$Ly6G$^-$ cells (IMs) were sorted by FACS. Sorted cells were stained for GRA6 (white), Ly6-B2 (green) and DAPI (blue) and examined by epifluorescence microscopy. Representative images of IMs containing RFP (red) and GRA6$^+$ (white) (left) and RFP$^+$GRA6$^-$ (right). Numbers indicate the proportion of RFP$^+$ IMs that are RFP$^+$GRA6$^+$, RFP$^+$GRA6$^-$. Experiment was performed 3 times with similar results and the compiled values for scored cells from all 3 experiments are presented. **(B-E)** Cre reporter bone

marrow cells were infected *in vitro* for 8hrs with live parasites expressing RFP and Cre. **(C)** Ly6-B2$^+$ cells that were GFP$^-$RFP$^-$, GFP$^+$RFP$^-$, GFP$^+$RFP$^+$ and GFP$^-$RFP$^+$ were sorted by FACS and relative expression of IFN-β was measured by qRT-PCR and normalized to GAPDH. IFN-β expression is shown relative to the IFN-β expression of sorted Ly6-B2$^+$GFP$^-$RFP$^+$ population. Data are compiled from 4 independent experiments. ($p=3.23\times10^{-9}$, F=175.58) Asterisk indicates pair of values that are statistically different based on a post hoc test. **(D)** Representative flow cytometry plots of RFP-containing Ly6-B2$^+$Ly6G$^-$ IMs (top) and Ly6-B2$^+$Ly6G$^+$ neutrophils (bottom) are shown. **(E)** Compiled data from flow cytometric analysis. Ratio of GFP$^+$RFP$^+$ to GFP$^-$RFP$^+$ in IMs and neutrophils are shown. Data are compiled from 4 independent experiments. The statistics were calculated using the unpaired t test. ($p=0.0122$) **(F)** Enriched Ly6-B2$^+$ (neutrophil and IMs) from WT bone marrow cells were cultured for 8hrs with indicated ratios of live or heat-killed parasites to IMs. Relative expression of IFN-β was measured by qRT-PCR and normalized to GAPDH. IFN-β expression is shown relative to the IFN-β expression of Ly6-B2$^+$ enriched sample infected with a ratio of parasites to IM of 1:1. Experiment was performed twice with similar results and data compiled from both experiments are shown. **(G)** Ly6G$^+$ (neutrophil enriched) and Ly6-B2$^+$ (neutrophil and IM enriched) bone marrow cells were untreated or treated with Latrunculin A for 30min and cultured for 8hrs with heat-killed (HK) parasites. Graph shows relative IFN-β expression of indicated samples (right). The relative expression of IFN-β was measured by qRT-PCR and normalized to GAPDH in each sample. IFN-β expression is shown relative to the Ly6-B2$^+$ population that were treated with heat-killed parasites. Representative flow cytometry plots of heath-killed parasites stimulated Ly6-B2$^+$ enriched samples, that were untreated and LatrunculinA treated from the same experiment are shown (left). Values are means (means ±SEM) of 3 independent experiments ($p=2.96\times10^{-7}$, F=43.07). **(H)** WT bone marrow cells were untreated or treated with Latrunculin A for 45min, cultured for 8hrs with heat-killed parasites, LPS or Pam3 and TNF-α production was measured by flow cytometry. Proportion of TNF-α producing IM following culture with indicated stimuli is shown. Experiment was performed twice and data from a representative experiment is shown. Average values of experimental triplicates are shown. Asterisks indicate pairs of values that are statistically different based on a post hoc Tukey test.

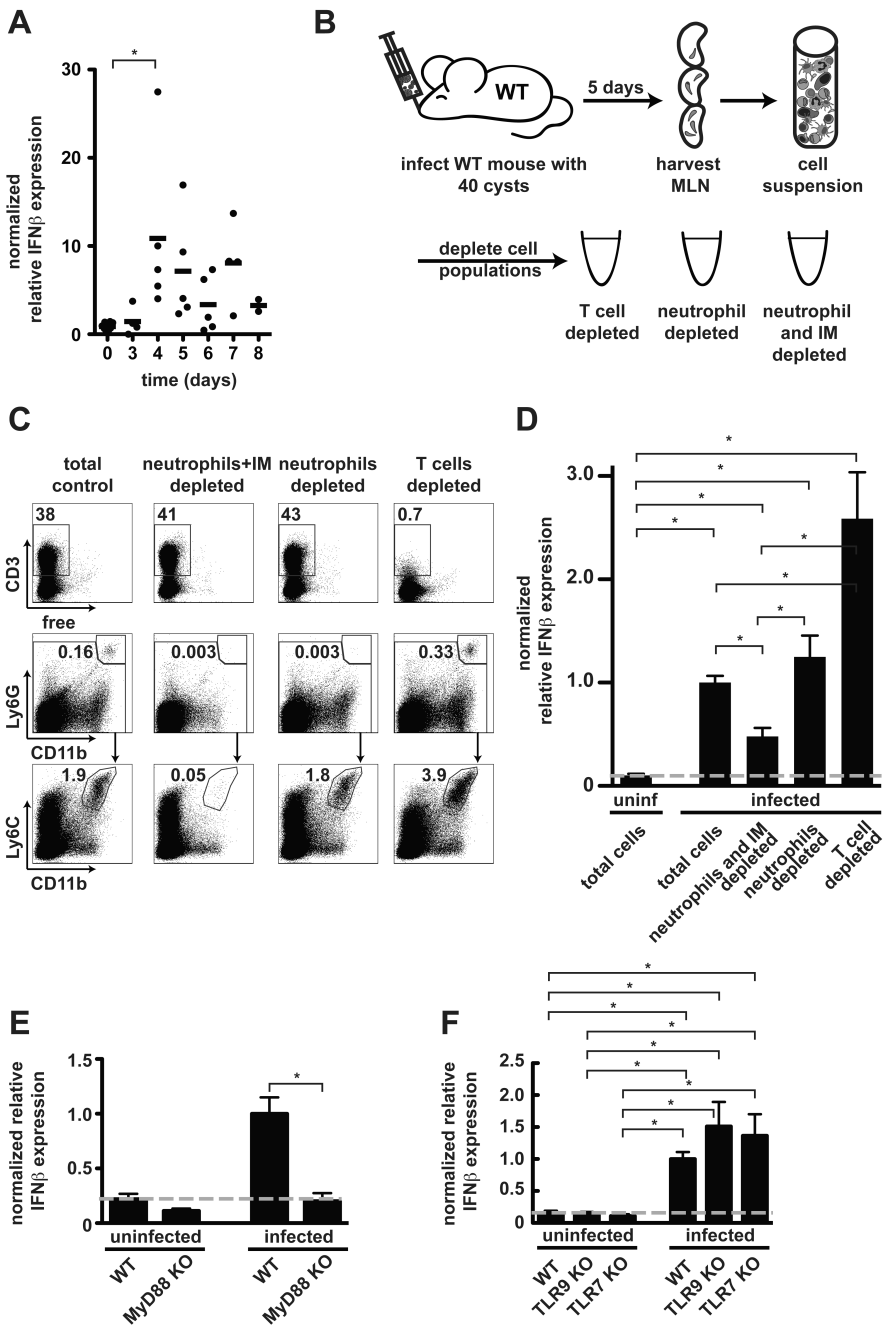

Figure 4. Inflammatory monocytes produce of IFN-β after *T. gondii in vivo* infection

(A) (C) Total RNA from WT MLNs were isolated at different time points (day 3-8) after oral infection, and expression of IFN-β was determined by qRT-PCR. IFN-β expression was normalized to GAPDH in each sample. **(A)** Experiment was performed twice and compiled data from both experiments are shown. Each dot represents an individual mouse (p=0.017966, F=3.15). **(B-D)** WT mice were orally infected and MLNs were harvested 5 days post infection. Single cell suspensions were stained with anti-Ly6G, Ly6-B2 or CD3 antibody, and the indicated populations were depleted. IFN-β expression of depleted and

non-depleted cell suspensions was determined by qRT-PCR normalized to GAPDH in each sample. The relative expression of IFN-β normalized to the average IFN-β expression of non-depleted sample on the day of analysis is shown. **(B)** Schematic of experimental set-up. **(C)** Representative flow cytometry plots of non-depleted control sample and samples depleted of each subset as indicated. The proportion of $CD3^+$ cells in depleted and non-depleted samples (top). The proportion of $Ly6G^+CD11b^+$ cells in depleted and non-depleted samples (middle). Bottom panel, $Ly6C^+CD11b^+$ cells in depleted and non-depleted samples. **(D)** Relative IFN-β expression in non-depleted samples or depleted samples is shown. Experiments were performed 6 times with 2 mice each (n=12) Values are means ±SEM of all experiments ($p=7.88\times10^{-8}$, F=40.84) **(E and F)** MLNs were harvested from WT and indicated KO mice, and 5 days post-infection, IFN-β expression was determined by qRT-PCR and normalized to GAPDH in each mouse. The expression of IFN-β is shown relative to the average IFN-β expression of infected WT mice on the day of analysis. Values are means ±SEM of combined experiments (at least 3 experiments per mutant mouse strain) (for E p=0.0065, F=4.72; for F $p=1.1\times10^{-12}$, F=45.14). Asterisks indicate pairs of values that are statistically different based on a post hoc Tukey test.

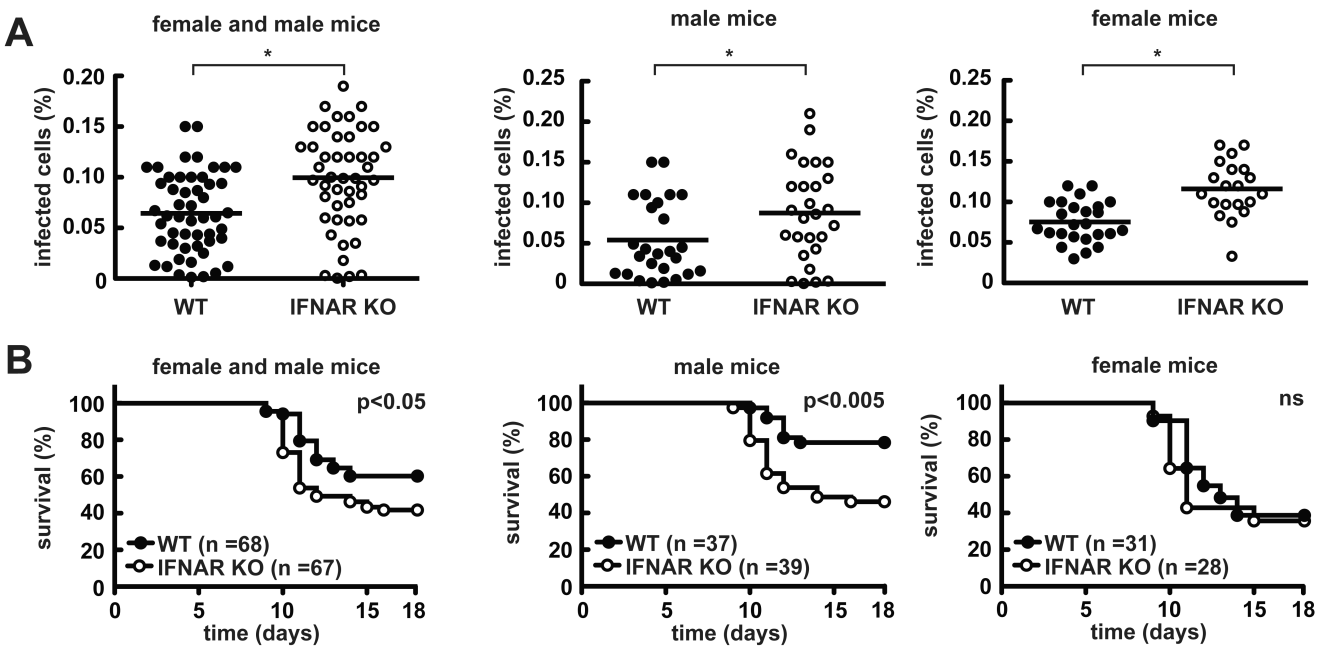

Figure 5. Impact of type I interferon following oral *Toxoplasma gondii* infection

(A) WT and IFNAR KO mice were orally infected with 40-50 cysts and mesenteric lymph nodes were analyzed 3 to 8 days post-infection. Each dot represents one mouse. Infected cells were enumerated by flow cytometry of mesenteric lymph nodes 5 days post infection. Graph shows combined data from at least 5 independent experiments, and is normalized to the average of infected WT mice on the day of analysis. The left graph shows combined data using male and female mice (left; $p<0.0002$), same data is shown using male mice (middle; $p=0.0274$) and female mice (right: $p<0.0001$). The statistics were calculated using the unpaired t test. **(B)** WT and IFNAR KO mice were orally infected with 40-50 *T. gondii* cysts and monitored for survival over 18 days. The left graph shows combined data of five independent survival experiments using male and female mice. The middle and right graph shows survival experiment using male and female mice from the same experiments. Presented are combined data of 5 independent experiments. The p value was calculated using the Mantel-Cox log-rank test.